

## PERFORMANCE EVALUATION OF AN EXTENDED KALMAN FILTER FOR STATE ESTIMATION OF A PSEUDO-2D THERMAL-ELECTROCHEMICAL LITHIUM-ION BATTERY MODEL

Shi Zhao, Adrien M. Bizeray, Stephen R. Duncan, David A. Howey\*

Department of Engineering Science, University of Oxford, Parks Road, Oxford OX1 3PJ, United Kingdom

Email: {shi.zhao, adrien.bizeray, stephen.duncan, david.howey}@eng.ox.ac.uk

### ABSTRACT

Fast and accurate state estimation is one of the major challenges for designing an advanced battery management system based on high-fidelity physics-based model. This paper evaluates the performance of a modified extended Kalman filter (EKF) for on-line state estimation of a pseudo-2D thermal-electrochemical model of a lithium-ion battery under a highly dynamic load with 16C peak current. The EKF estimation on the full model is shown to be significantly more accurate ( $< 1\%$  error on SOC) than that on the single-particle model (10% error on SOC). The efficiency of the EKF can be improved by reducing the order of the discretised model while maintaining a high level of accuracy. It is also shown that low noise level in the voltage measurement is critical for accurate state estimation.

### INTRODUCTION

Lithium-ion batteries are the cell chemistry of choice for electric and hybrid electric vehicle applications due to their high energy and power density. However, individual cells must be carefully monitored and controlled to ensure safe and reliable operation of the battery pack. This is performed by an embedded system, so called battery management system (BMS), consisting of hardware and embedded control algorithms. The use of numerous cells in large battery packs with long lifetime requirements in automotive and other applications requires developing novel advanced BMSs for improved safety and reliability. Particularly, BMSs use a battery dynamic model to infer internal states, such as state-of-charge (SOC) and state-of-health (SOH), from

available measurements of voltage, current and surface temperature. Simplistic empirically-fitted models, such as equivalent circuit models (ECMs), are usually employed due to their low computational requirements but such data-driven approaches are usually invalid under extreme conditions (high current, extreme temperatures, highly dynamic load...). In addition, estimation and prediction of capacity and power fade due to degradation remain challenging due the lack of physical meaning of such data-driven models.

Instead, high-fidelity physics-based models describing transport, kinetics and thermodynamics phenomena within the cell could be used in novel BMSs for accurate states monitoring and control. In addition, such first-principle models can be coupled to degradation models directly by virtue of the physical significance of model parameters. The so-called pseudo-two dimensional (P2D) model developed by Newman and his coworkers [1] has been widely used for battery design but not embedded applications because of its high computational cost. Several attempts have been made at reducing the computational burden of the P2D model in recent years for control and estimation purposes. State estimation algorithms based on simplified physics-based models such as the single-particle model (SPM) and similar approximations have been investigated [2, 3], but are inherently limited to low C-rate operation ( $< 2C$ ). Model-order reduction techniques have also been used to derive low-order models from the P2D model [4, 5], but the physical meanings of reduced-model parameters may be difficult to interpret.

Spectral methods have recently been used for the solution of the full P2D model [6–8]. Compared to finite-difference or finite-element methods, the spatial discretisation of the P2D

---

\*Address all correspondence to this author.

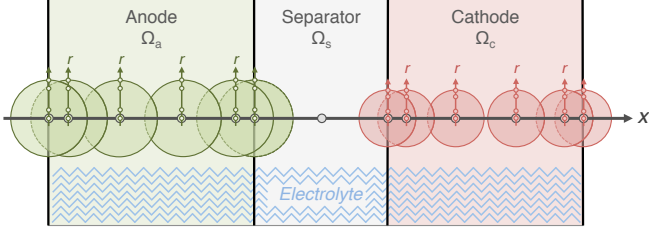


Figure 1. SCHEMATIC OF THE CELL COMPUTATIONAL DOMAINS.

model using spectral methods, such as orthogonal collocation, results in a much lower order model and faster solution (reduced by a factor of  $10 \sim 100$ ), while maintaining the solution accuracy and the physical meaning of model parameters [6, 8]. In a previous work [9], we discussed the implementation of an EKF for the state estimation of the full P2D model solved using Chebyshev orthogonal collocation. This paper evaluates the performance of this state estimation algorithm with reduced number of discretisation nodes and under different levels of measurement noise.

## BATTERY DYNAMIC MODEL

### Thermal-Electrochemical P2D Model

The battery model considered is the P2D electrochemical model describing lithium transport, reaction kinetics and thermodynamics at the electrode level, coupled to a bulk thermal model describing the average cell temperature.

During discharge, lithium stored in the anode active material is released as ions into the electrolyte and migrates to the cathode where it is re-inserted into the active material. Simultaneously, an electric current is created by electrons travelling from the anode to the cathode through the external circuit to maintain electroneutrality. This process is reversed during charging. The P2D model describes the evolution of lithium concentration and electric potential across the cell thickness ( $x$ -coordinates) on three domains, anode  $\Omega_a$ , separator  $\Omega_s$  and cathode  $\Omega_c$  (Fig. 1), where the electrolyte phase and the solid phase are treated as superimposed continua using the porous electrode theory [10]. The diffusion of lithium in the porous active material of the electrodes is described by considering solid-phase particles distributed across the cell thickness, giving rise to the model pseudo-second dimension ( $r$ -coordinates). The thermal-P2D model therefore consists of a set of coupled partial differential-algebraic equations (PDAEs) composed of diffusion and Ohm's law equations solved on the  $x$ -coordinates, spherical diffusion equations solved on the  $r$ -coordinates and a zero-dimensional heat equation. Due to space limitations, these equations are not given here. The reader is referred to [9] for the details.

An analytical solution for such a complex problem is not available and numerical methods are employed to spatially dis-

cretise the equations in the  $x$ - and  $r$ -directions. The discretised P2D model consists of a system of ODEs and DAEs that can be integrated using a standard time-adaptive ODE/DAE solver such as MATLAB's *ode15s* [11]. The finite difference method has been commonly used to discretise the P2D model in space but this requires a significant number of discrete nodes and therefore results in a large system of equations. In this paper, the electrochemical P2D model is discretised using a class of spectral methods called Chebyshev orthogonal collocation that results in a much smaller system of equations compared to finite difference for a similar accuracy [12]. The details of the discretisation approach can be found in [8].

### DAEs State-Space Notation

The P2D model discretised by orthogonal collocation consists of a set of nonlinear differential-algebraic equations (DAEs). Using a state-space representation, the model can be conveniently written as

$$\dot{\mathbf{x}} = \mathbf{f}(\mathbf{x}, \mathbf{z}, u) \quad (1)$$

$$\mathbf{0} = \mathbf{g}(\mathbf{x}, \mathbf{z}, u) \quad (2)$$

$$\mathbf{y} = H_x \mathbf{x} + H_z \mathbf{z} + H_u u \quad (3)$$

where the functions  $\mathbf{f}$  and  $\mathbf{g}$  are nonlinear mapping functions derived from the discretised model equations. The state vector  $\mathbf{x} = [\bar{c}_s, c_e, T]^T \in \mathbb{R}^{n_x}$  associated with the differential equations contains the value at the collocation points of the solid-phase concentration  $\bar{c}_s$  and the electrolyte concentration  $c_e$ , as well as the bulk temperature  $T$ . The state vector  $\mathbf{z} = [\mathbf{j}^{Li}, \phi_{s,c}^0, \phi_{s,a}^0]^T \in \mathbb{R}^{n_z}$  associated with the algebraic equations contains the value of the volumetric reaction rate  $\mathbf{j}^{Li}$  at the collocation points and the solid-phase electric potential at the cathode and anode current collector  $\phi_{s,c}^0$  and  $\phi_{s,a}^0$  respectively. The measurement vector  $\mathbf{y} = [V \ T]^T$  containing the value of the voltage  $V$  and the temperature  $T$  is computed from the differential and algebraic state vectors according to the measurement equation (3) where the input  $u$  is the applied current.

## MODIFIED EXTENDED KALMAN FILTER

### Model Linearisation

A modified EKF described in [13] is applied to the nonlinear DAE state-space model. Define  $\tilde{\mathbf{x}} = \mathbf{x} - \hat{\mathbf{x}}$ ,  $\tilde{\mathbf{z}} = \mathbf{z} - \hat{\mathbf{z}}$  and  $\tilde{u} = u - \hat{u}$  where  $(\hat{\mathbf{x}}, \hat{\mathbf{z}}, \hat{u})$  is the linearisation point. Assuming that the functions  $\mathbf{f}$  and  $\mathbf{g}$  are sufficiently differentiable, linearisation of the differential equation and the algebraic equation about the current state estimate  $[\hat{\mathbf{x}}, \hat{\mathbf{z}}]^T$  gives

$$\dot{\tilde{\mathbf{x}}} = A\tilde{\mathbf{x}} + B\tilde{u} \quad (4)$$

where  $A = \mathbf{f}_x - \mathbf{f}_z \mathbf{g}_z^{-1} \mathbf{g}_x$  and  $B = \mathbf{f}_u - \mathbf{f}_z \mathbf{g}_z^{-1} \mathbf{g}_u$ , while  $\mathbf{f}_i$  and  $\mathbf{g}_i$  denote the partial derivative of  $\mathbf{f}$  and  $\mathbf{g}$  respectively with respect to the variable  $i = \{\mathbf{x}, \mathbf{z}, u\}$  evaluated at the current state estimate  $[\hat{\mathbf{x}}, \hat{\mathbf{z}}]^T$ .

Define  $\hat{\mathbf{y}} = H_x \hat{\mathbf{x}} + H_z \hat{\mathbf{z}} + H_u \hat{u}$  and  $\tilde{\mathbf{y}} = \mathbf{y} - \hat{\mathbf{y}}$ . Linearisation of the output equation about  $\hat{\mathbf{y}}$  gives

$$\tilde{\mathbf{y}} = C \tilde{\mathbf{x}} + D \tilde{u} \quad (5)$$

where  $C = H_x - H_z \mathbf{g}_z^{-1} \mathbf{g}_x$  and  $D = H_u - H_z \mathbf{g}_z^{-1} \mathbf{g}_u$ .

### EKF Implementation

With the linearised state-space model at hand, it is straightforward to implement the modified EKF. The algorithm at every time step is summarised as follows:

1. The current state estimation is projected forward by using the MATLAB solver for DAEs *ode15s*.
2. The state covariance matrix for the differential states is updated by using the matrix  $A$  in the linearised model.
3. The Kalman gain for the differential states is calculated.
4. The *a posteriori* differential state estimate and the corresponding state covariance matrix are computed.
5. The consistent *a posteriori* algebraic state estimate is obtained from the *a posteriori* differential state estimate and the input using the MATLAB *fsolve* function.

Note that at every time step, only the differential states  $\mathbf{x}$  are updated by the Kalman gain. Once the *a posteriori* differential state estimation is obtained, the consistent algebraic state estimate needs to be solved from the algebraic equation (2). This turns out to be the most time-consuming step of the EKF. In fact, step 5 takes about 60% of the computation time at each time step. For this reason, the unscented Kalman filter (UKF) is not a suitable choice for state estimation of the model, although the system is nonlinear and the UKF may propagate the state covariance matrix more accurately than the EKF. Specifically, due to the need to find the consistent algebraic states for all the  $2n_x + 1$  sigma points at every time step where  $n_x$  is the number of differential states and is of the order of 100, it would take significantly more time for the UKF to estimate the states. Thus it is not realistic to run the UKF in real-time.

The Jacobian matrices in the linearised state space model (4) and (5) are computed using the complex step differentiation method, which is more accurate than using the classical finite difference method [14]. Numerical calculation of the Jacobian matrices takes about 25% of the computation time. We are currently exploring the possibility to improve both the efficiency and accuracy by deriving these matrices analytically.

The initial state error covariance matrix  $P_0$  is computed numerically from the model states solved by integration under

various inputs and initial conditions. The structure of such a  $P_0$  accounts for the spatial correlation of the system states such that the law of conservation of charge is not violated.

### SIMULATION RESULTS AND DISCUSSION

This section presents simulation results illustrating the performance of the modified EKF estimating the states of the full thermal-electrochemical model. Ideally, the performance of the EKF should be evaluated against real experimental data, but due to the difficulties in identifying the parameters and verifying *in situ* the internal states in a real battery, the common approach in the literature is to compare the results of the EKF with the simulation results of the physics-based model [2, 15]. This approach is employed in this paper and the data used as the reference are obtained by integrating the thermal-electrochemical model from 100% SOC until the 2V minimum cut-off voltage under the dynamic current excitation profile generated from the Combined ARTEMIS Driving Cycle (CADC) [16]. The maximum C-rate for the CADC is 16C. The chosen numbers of collocation nodes in the anode, separator and cathode are  $N_a = 6$ ,  $N_s = 3$  and  $N_c = 6$  respectively and the number of collocation nodes in each particle of both electrodes is  $N_p = 15$ . The simulation was carried out on a desktop computer using a 3.40 GHz processor with 8 GB RAM. The accuracy of the data has been confirmed by a comparison with the results generated using the commercial finite-element software COMSOL Multiphysics with much higher discretisation resolutions [8].

The EKF initial guess on states assumed a cell at equilibrium with an error on both the anode and cathode SOC of 30%. The initial error on the temperature was set to 10°C. The standard deviations for the generation of the additive Gaussian white measurement noise were set to  $\sigma_V = 10\text{mV}$  and  $\sigma_T = 0.5\text{K}$  for the voltage and temperature respectively. No process noise accounting for modelling error was added.

Numerical experiments show that the anode bulk SOC and the electrolyte concentration estimated by the EKF rapidly converge to the actual values, as seen in Fig. 2 and Fig. 3, where the EKF was started at  $t = 60\text{s}$ . Due to charge conservation, the result on the cathode bulk SOC is almost identical to that on the anode bulk SOC. As shown in [9], the convergence behaviour of the EKF started at different times with different initial conditions is very similar. With a time step of 5s, the EKF was solved in 0.6s of computation per second of simulation on average on the desktop computer previously mentioned. Note that as  $N_a = 6$ ,  $N_s = 3$ ,  $N_c = 6$  and  $N_p = 15$ , the system model has 166 differential states and 14 algebraic states.

### Number of Collocation Nodes

Although the EKF can estimate the states of the system in real-time, it is still desirable to reduce the computation time

as much as possible without compromising the accuracy of the estimation much. One possible way to achieve this goal is to reduce the number of collocation nodes used in the EKF. This certainly can reduce the computation time, but it remains to show that the EKF still gives sufficiently accurate estimation.

If  $N_p$  is reduced to 8, the number of the algebraic states remains unchanged, but the number of the differential states is reduced to 82. Numerical experiments show that the estimation time is reduced by a third. The performance of the reduced-order EKF compared against the reference data is illustrated in Fig. 2 and Fig. 3. The anode bulk SOC and the electrolyte concentration can still be estimated accurately, although the convergence is slower, which is expected. Similarly, if  $N_p$  is reduced even further to 6, it is even faster to run the EKF, which comes at the cost of less accurate estimation and slower convergence.

### Comparison with EKF Based on SPM

The P2D model is simplified to a SPM by reducing the number of particles in each of the electrodes to one (i.e.,  $N_a = 1$  and  $N_c = 1$ ) and assuming that the electrolyte concentration has no spatial variations. As the discretised SPM is an ODE model rather than a DAE model, it takes considerably less efforts to design and run an EKF for state estimation. The computation time of the estimation based on the SPM is only about 1/40 of that using the full P2D model with  $N_a = 6$ ,  $N_s = 3$ ,  $N_c = 6$  and  $N_p = 15$ . However, the accuracy of the estimation based on the SPM under the CADC is vastly inferior to that given by the EKF based on the full P2D model, as can be seen in Fig. 2. The error on the SOC estimation by the EKF based on SPM is typically around 10%, although  $N_p$  is set to 15 in the computation. Moreover, such an EKF is not able to estimate the electrolyte concentration due to the assumption of no spatial variations in the SPM.

### Measurement Noise Level

So far the measurement noise is set to  $\sigma_V = 10\text{mV}$  and  $\sigma_T = 0.5\text{K}$ . This subsection studies the performance of the EKF (based on the full P2D model) under different levels of noise. The focus is first restricted to the impact of voltage measurement noise. Fig. 4 shows the accuracy of the state estimation by the EKF deteriorates when the voltage noise level is increased to  $\sigma_V = 20\text{mV}$  and  $\sigma_V = 50\text{mV}$  while the measurement noise covariance matrix in the EKF is adjusted accordingly and  $\sigma_T$  is fixed at  $0.5\text{K}$ . The numbers of collocation nodes used in the computations are  $N_a = 6$ ,  $N_s = 3$ ,  $N_c = 6$  and  $N_p = 15$ . The results demonstrate that noisier voltage measurement makes the state estimation less reliable. By contrast, similar numerical experiments show that the accuracy of state estimation is not as sensitive to noisy temperature measurement.

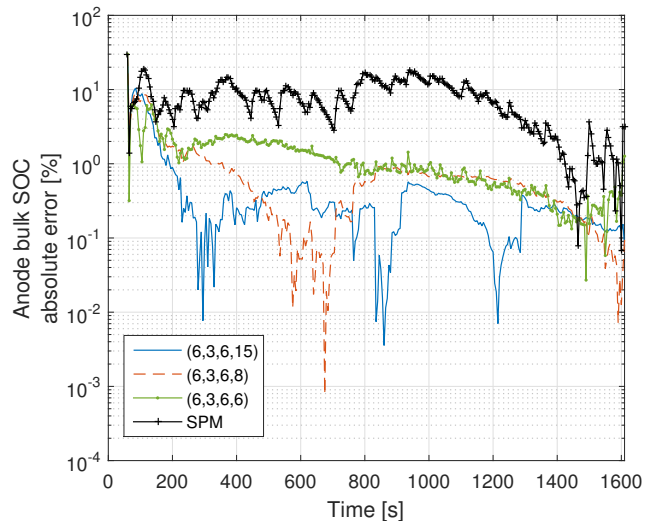


Figure 2. ERROR ON ANODE BULK SOC ESTIMATED BY THE EKF WITH REDUCED NUMBERS OF DISCRETISATION NODES  $(N_a, N_s, N_c, N_p)$  AND BY THE EKF BASED ON SPM COMPARED TO THE HIGH-FIDELITY REFERENCE CASE (6,3,6,15).

### CONCLUSION

The performance of a modified EKF for state estimation of a pseudo-2D thermal-electrochemical lithium-ion battery model is evaluated against high-fidelity simulation data. The EKF estimation on the full model is shown to be significantly more accurate than that on the SPM. This is important in high C-rate applications where accurate state estimation is required, such as fast charging and hybrid vehicle supervisory control systems. The computation burden can be reduced by employing a reduced-order EKF. Relatively noise free voltage measurement is critical for the performance of the EKF.

### ACKNOWLEDGMENT

S. Zhao is funded through the RCUK Energy Programmes STABLE-NET project (ref. EP/L014343/1). A.M. Bizeray is funded by Samsung Electronics Co. Ltd. through a Global Research Outreach program in collaboration with the Samsung Advanced Institute of Technology.

### REFERENCES

- [1] Doyle, M., Fuller, T. F., and Newman, J., 1993. "Modeling of Galvanostatic Charge and Discharge of the Lithium/Polymer/Insertion Cell". *Journal of The Electrochemical Society*, **140**(6), p. 1526.
- [2] Santhanagopalan, S., and White, R. E., 2006. "Online

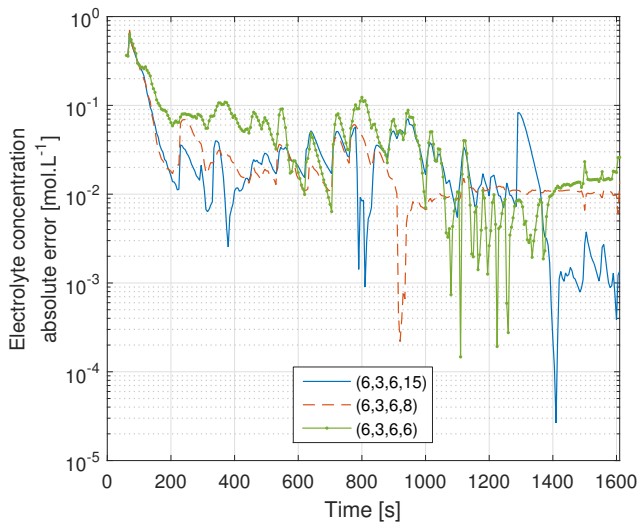


Figure 3. ERROR ON THE ELECTROLYTE CONCENTRATION AT THE ANODE CURRENT COLLECTOR ESTIMATED BY THE EKF WITH REDUCED NUMBERS OF DISCRETISATION NODES ( $N_a, N_s, N_c, N_p$ ) COMPARED TO THE HIGH-FIDELITY REFERENCE CASE (6,3,6,15).

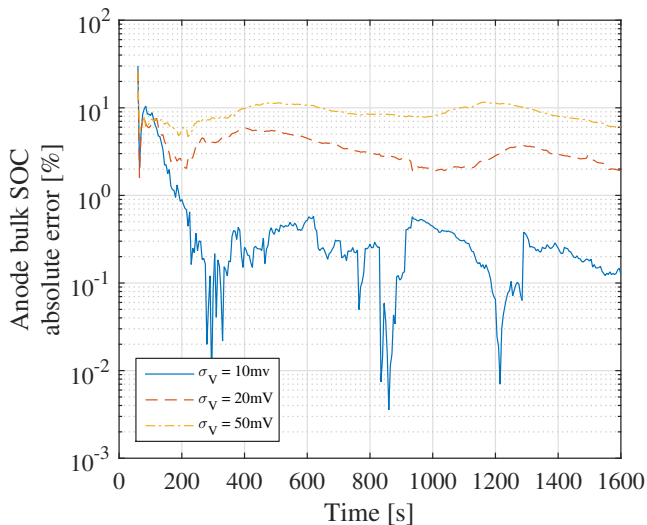


Figure 4. ERROR ON ANODE BULK SOC COMPUTED BY THE EKF FOR DIFFERENT LEVELS OF VOLTAGE MEASUREMENT NOISE.

estimation of the state of charge of a lithium ion cell”. *Journal of Power Sources*, **161**(2), Oct., pp. 1346–1355.

[3] Moura, S. J., Chaturvedi, N. A., and Krstić, M., 2013. “Adaptive Partial Differential Equation Observer for Battery State-of-Charge/State-of-Health Estimation Via an Electrochemical Model”. *Journal of Dynamic Systems, Measurement, and Control*, **136**(1), Oct., p. 011015.

[4] Smith, K., Rahn, C. D., and Wang, C.-Y., 2008. “Model-based electrochemical estimation of lithium-ion batteries”. *2008 IEEE International Conference on Control Applications*(1), pp. 714–719.

[5] Stetzel, K. D., Aldrich, L. L., Trimboli, M. S., and Plett, G. L., 2015. “Electrochemical state and internal variables estimation using a reduced-order physics-based model of a lithium-ion cell and an extended Kalman filter”. *Journal of Power Sources*, **278**, pp. 490–505.

[6] Northrop, P. W. C., Ramadesigan, V., De, S., and Subramanian, V. R., 2011. “Coordinate Transformation, Orthogonal Collocation, Model Reformulation and Simulation of Electrochemical-Thermal Behavior of Lithium-Ion Battery Stacks”. *Journal of The Electrochemical Society*, **158**(12), p. A1461.

[7] Cai, L., and White, R. E., 2012. “Lithium ion cell modeling using orthogonal collocation on finite elements”. *Journal of Power Sources*, **217**, Nov., pp. 248–255.

[8] Bizeray, A., Duncan, S., and Howey, D., 2013. “Advanced battery management systems using fast electrochemical modelling”. In *Hybrid and Electric Vehicles Conference 2013 (HEVC 2013)*, Institution of Engineering and Technology, pp. 2.2–2.2.

[9] Bizeray, A. M., Zhao, S., Duncan, S. R., and Howey, D. A., 2015. “Lithium-ion battery thermal-electrochemical model-based state estimation using orthogonal collocation and a modified extended Kalman filter”. *Journal of Power Sources*, **296**, Nov.

[10] Newman, J., and Tiedemann, W., 1975. “Porous-electrode theory with battery applications”. *AIChE Journal*, **21**(1), Jan., pp. 25–41.

[11] Shampine, L. F., Reichelt, M. W., and Kierzenka, J. A., 1999. “Solving Index-1 DAEs in MATLAB and Simulink”. *SIAM Review*, **41**(3), Jan., pp. 538–552.

[12] Trefethen, L. N., 2000. *Spectral Methods in MATLAB*. SIAM.

[13] Becerra, V. M., Roberts, P. D., and Griffiths, G. W., 2001. “Applying the extended Kalman filter to systems described by nonlinear differential-algebraic equations”. *Control Engineering Practice*, **9**, pp. 267–281.

[14] Squire, W., and Trapp, G., 1998. “Using complex variables to estimate derivatives of real functions”. *SIAM Review*, **40**(1), pp. 110–112.

[15] Suthar, B., Ramadesigan, V., Northrop, P. W. C., Gopaluni, B., Santhanagopalan, S., Braatz, R. D., and Subramanian, V. R., 2013. “Optimal Control and State Estimation of Lithium-ion Batteries Using Reformulated Models”. *American Control Conference (ACC), 2013*, pp. 5350–5355.

[16] André, M., 2004. “The ARTEMIS European driving cycles for measuring car pollutant emissions”. *Science of the Total Environment*, **334-335**, pp. 73–84.